Available online at www.sciencedirect.com
SCIENCE DIRECT
Biochimica et Biophysica Acta 1716 (2005) 49 – 58
BIOCHIMICA ET BIOPHYSICA ACTA
BBA
http://www.elsevier.com/locate/bba

# Coverage-dependent changes of cytochrome *c* transverse location in phospholipid membranes revealed by FRET☆

Yegor A. Domanov [a,*], Julian G. Molotkovsky [b], Galyna P. Gorbenko [a]

[a] *Department of Biological and Medical Physics, V. N. Karazin Kharkiv National University, 4 Svobody Sq., Kharkiv 61077, Ukraine*
[b] *Shemyakin-Ovchinnikov Institute of Bioorganic Chemistry, Russian Academy of Sciences, 16/10 Miklukho-Maklaya Str., Moscow 117997, Russia*

Received 10 June 2005; received in revised form 28 July 2005; accepted 1 September 2005

**Abstract**

The method of fluorescence resonance energy transfer (FRET) has been employed to monitor cytochrome *c* interaction with bilayer phospholipid membranes. Liposomes composed of phosphatidylcholine and varying amounts of anionic lipid cardiolipin (CL) were used as model membranes. Trace amount of fluorescent lipid derivative, anthrylvinyl-phosphatidylcholine was incorporated into the membranes to serve energy donor for heme moiety of cytochrome *c*. Energy transfer efficiency was measured at different lipid and protein concentrations to obtain extensive set of data, which were further analyzed globally in terms of adequate models of protein adsorption and energy transfer on the membrane surface. It has been found that the cytochrome *c* association with membranes containing 10 mol% CL can be described in terms of equilibrium binding model (yielding dissociation constant $K_d$=0.2–0.4 μM and stoichiometry $n$=11–13 lipid molecules per protein binding site) combined with FRET model assuming uniform acceptor distribution with the distance of 3.5–3.6 nm between the bilayer midplane and heme moiety of cytochrome *c*. However, increasing the CL content to 20 or 40 mol% (at low ionic strength) resulted in a different behavior of FRET profiles, inconsistent with the concepts of equilibrium adsorption of cytochrome *c* at the membrane surface and/or uniform acceptor distribution. To explain this fact, several possibilities are analyzed, including cytochrome *c*-induced formation of non-bilayer structures and clusters of charged lipids, or changes in the depth of cytochrome *c* penetration into the bilayer depending on the protein surface density. Additional control experiments have shown that only the latter process can explain the peculiar concentration dependences of FRET at high CL content.


*Keywords:* Cytochrome *c*; FRET; Membrane insertion; Quantitative analysis; Cardiolipin

## 1. Introduction

Cytochrome *c* (cyt *c*) is a peripheral membrane protein found in the intermembrane space of mitochondria. With Fe ion in its heme moiety switching between $Fe^{2+}$ (ferro) and $Fe^{+3}$ (ferri) redox states, this protein transfers electrons from cytochrome $bc_1$ complex to cytochrome *c* oxidase in the respiratory chain of the inner mitochondrial membrane [1]. Since both redox partners of cyt *c* are membrane-spanning protein complexes, cyt *c*–membrane interactions play essential role in the respiration process. It has been shown that the electron transport is mediated by the cyt *c* diffusion—either in three dimensions, in the intermembrane space, or in two dimensions, when the protein is bound to the inner mitochondrial membrane, the mode of diffusion being determined by the ionic strength of the medium [2]. In addition to this conventional function, the problem of cyt *c* interaction with phospholipid membranes is related to two other very important physiological and pathological processes. Firstly, cyt *c* release from mitochondria into the cytosol triggers apoptosis or programmed cell death [3]. Apoptosis is involved in embryo development, elimination of damaged cells, and maintenance of cell homeostasis. Secondly, recent findings indicate that cyt *c* belongs to the group of proteins that have ability for membrane-induced formation of amyloid fibers [4]. Amyloid deposits in tissues are known to accompany a number of severe illnesses such as Alzheimer's disease, Parkinson's disease, type II diabetes, etc.

☆ Presented at the 5th International Conference on Biological Physics, August, 2004, Göteborg, Sweden.

* Corresponding author. Institute of Biomedicine/Biochemistry, Helsinki University, P.O. Box 63 (Haartmaninkatu 8), 00014 Helsinki, Finland. Tel.: +358 45 1332883; fax: +358 9 19125444.
*E-mail address:* egoord@yahoo.com (Y.A. Domanov).

0005-2736/$ - see front matter © 2005 Elsevier B.V. All rights reserved.
doi:10.1016/j.bbamem.2005.09.002

The interactions of cyt *c* with phospholipid membranes have been extensively studied with a variety of techniques, both in mitochondrial membranes [5] and model systems such as liposomes [6], monolayers at the air–water interface [7], or solid-supported bilayers [8,9]. Membranes incorporating anionic lipids are used in the majority of studies, since mitochondrial membranes are known to be rich in negatively charged lipids, particularly, cardiolipin [10]. Initial binding of the protein to the membrane is electrostatically driven due to the net positive charge of cyt *c*. However, significant role of hydrophobic interactions [8,11] and hydrogen bonding [12] under specific conditions has also been suggested.

In the present study, we employed fluorescence resonance energy transfer (FRET) from anthrylvinyl phospholipid derivatives to heme group of cyt *c* in order to obtain quantitative information about cyt *c* transverse location in the model membranes composed of egg phosphatidylcholine and varying amounts of cardiolipin. It was found that under the conditions of low ionic strength and high cardiolipin content (>20 mol% of total lipid) changes in the protein surface density on the membrane can induce partial insertion of cyt *c* deeper into the bilayer.

## 2. Theory

Quantitative analysis of FRET data was performed using the model of energy transfer between donors and acceptors uniformly distributed in the planes parallel to the membrane surface as described in detail elsewhere [13,14]. Relative quantum yield of the donor, which is observed experimentally, can be represented as

$$Q_r = \frac{F_{DA}}{F_D} = \frac{1}{\tau_D}\int_0^\infty \exp(-t/\tau_D)(I(t))^N dt, \quad (1)$$

where $F_{DA}$ and $F_D$ are the donor fluorescence intensities (e.g., at the emission maximum) in the presence and in the absence of acceptors, respectively, $\tau_D$ is the donor excitation lifetime, and

$$I(t) = \int_{d_c}^{R_d} \exp\left[-t/\tau_D (R_0/R)^6\right] W(R) dR \quad (2)$$

is the additional donor decay due to FRET to acceptors (Fig. 1). Here, $d_c$ is the distance between the acceptor plane and the bilayer midplane, $R_d$ is the distance beyond which energy transfer is negligible ($R_d \geq 3R_0$), $R_0$ is the Förster radius, and $W(R)dR$ is the probability of finding an acceptor at the distance between $R$ and $R+dR$ from the donor. $N$ is the number of acceptors located within the distance $R_d$ from the donor. For the geometry shown in Fig. 1

$$W(R)dR = \frac{2RdR}{R_d^2 - d_c^2} \quad (3)$$

and

$$N = \pi C_A^s \left[R_d^2 - d_c^2\right]. \quad (4)$$

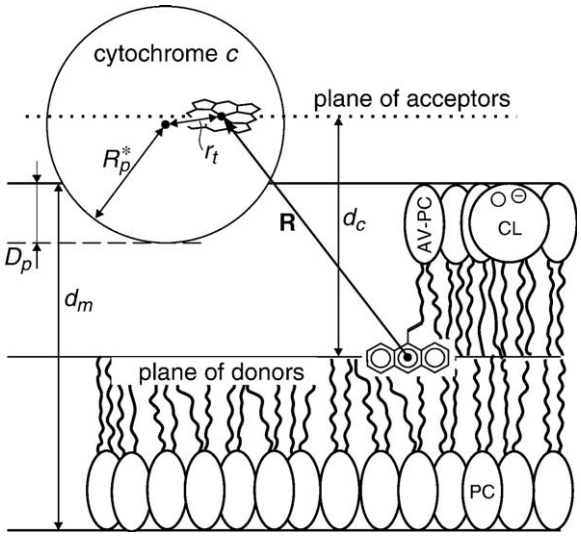


Fig. 1. Scheme of cytochrome *c* bound to phospholipid membrane. Locations of energy donors (anthrylvinyl moieties of fluorescent lipid derivatives) and acceptors (heme groups in cytochrome *c*) are shown together with the geometric parameters that are used in theoretical calculations (see text).

Here $C_A^s$ is the acceptor surface concentration related to the molar concentrations of bound acceptor, $B$, and accessible lipid, $L_{acs}$:

$$C_A^s = \frac{B}{L_{acs}\sum f_j S_j}, \quad (5)$$

$f_j$ and $S_j$ being the mole fraction and mean area per molecule of the $j$-th lipid species constituting the membrane, respectively.

In order to relate the concentration of bound acceptor (protein) to the experimental variables, $L_{acs}$ and $P$ ($P$ being the total protein concentration), the above model was coupled to the protein adsorption isotherm. Here, we use the isotherm derived within the framework of scaled particle theory (SPT, [15]):

$$K_d^{-1}(P-B) = \frac{\theta}{1-\theta}\exp\left[\frac{3\theta}{1-\theta} + \left(\frac{\theta}{1-\theta}\right)^2\right], \quad (6)$$

where $\theta = n_{pm}B/L_{acs}$ is the fraction of membrane surface covered with protein, $n_{pm}$ is the number of lipid molecules covered by one protein molecule.

## 3. Materials and methods

### 3.1. Materials

All experiments were carried out in 5 mM Na-phosphate buffer, pH 7.4. In some cases, NaCl was added to increase the ionic strength of the medium. Phosphatidylcholine (PC) and phosphatidylglycerol (PG) from egg yolk and cardiolipin (CL) from bovine heart were purchased from Sigma (Steinheim, Germany). Horse heart cytochrome *c* (cyt *c*) was from Fluka (Buchs, Switzerland). Based on spectrophotometric measurements, the protein was mainly in the oxidized form (>90%). Protein concentration was determined spectrophotometrically using $\varepsilon_{406} = 1.05 \times 10^5$ $M^{-1}$ $cm^{-1}$.

### 3.2. Preparation of liposomes

Large unilamellar vesicles were prepared by ethanol injection method [16]. Ethanol solutions of PC and CL (or PG) were mixed in necessary ratio and rapidly injected into the buffer solution under rapid stirring. Trace amount of

fluorescent lipid (<0.35 mol% of total lipid) was added to the lipid mixture before injection. After injection, ethanol (<7%) was removed from the liposome suspension by extensive dialysis. All volumes were thoroughly measured and used for calculating the lipid concentration in liposome preparations. Total lipid concentration was also checked by the method of Bartlett [17]. Liposomes were stored at +5 °C and used within 2 days of preparation.

### 3.3. Fluorescent lipids

Fluorescent lipid analogues used here as energy donors, 1-acyl-2-[12-(9-anthryl)-11-*trans*-dodecenoyl]-*sn*-glycero-3-phosphocholine (anthrylvinyl-phosphatidylcholine, AV-PC) and 1-acyl-2-[12-(9-anthryl)-11-*trans*-dodecenoyl]-*sn*-glycero-3-phospho-1-*rac*-glycerol (anthrylvinyl-phosphatidylglycerol, AV-PG) were synthesized as described previously [18,19]. Their chemical structures are shown in Fig. 2. AV-PC and AV-PG are chemically and photostable, have a high quantum yield (~0.8 in liposomes) and emission wavelength position and quantum yield independent of the environment polarity [20]. Due to its non-polar nature, the anthrylvinyl group resides in the hydrophobic region of the membrane and causes only minor perturbation of the bilayer. $^1$H-NMR data [20] suggest that the antrylvinyl rings lie perpendicular to the bilayer plane (see Fig. 1) close to the bilayer midplane. Finally, AV has considerable emission in Soret band (Fig. 3) making it an effective energy donor for heme proteins.

### 3.4. Fluorescence measurements

Fluorescence measurements were made using Hitachi M850 or Hitachi F-4010 spectrofluorometer (Hitachi Corp., Japan). Fluorescence of AV-labeled phospholipids was excited at 375 nm and recorded at 430 nm with slit widths set to 5 nm. All measurements were performed at 20 °C. Absorption spectra were recorded with CM 2203 combined spectrometer (SOLAR, Belarus). pH of solutions was controlled using EV-74 ion meter (ZIP, Russia).

The relative quantum yield of donor was determined as a ratio of donor intensities in the presence and in the absence of acceptor. 1 mL of fluorescent liposome suspension was mixed in standard quartz cuvette (1 × 1 cm) with 0.2 mL of buffer or cyt *c* solution to obtain different combinations of lipid and protein concentrations.

Overall absorption at the excitation and emission wavelengths for all samples used in fluorescence measurements was below 0.4 in 1-cm cuvette. To correct the fluorescence intensity for the inner filter effect, two approaches were utilized. First, correction coefficients $K$ were calculated using the following simplified formula [21]:

$$K = \frac{F_{corr}}{F_{obs}} = 10^{\frac{A(\lambda ex)+A(\lambda em)}{2}}, \quad (7)$$

where $F_{corr}$ is the corrected intensity, $F_{obs}$ is the observed intensity, $A(\lambda_{em})$ is the absorption at the excitation wavelength, and $A(\lambda_{em})$ is the absorption at the emission wavelength. Second, to verify the coefficients calculated using Eq. (7), in some measurements empirical correction coefficients were also obtained by recording the fluorescence intensity for identical samples at a high ionic strength (0.5 M NaCl). Under such conditions, no association of cytochrome *c* with phospholipids occurs (e.g., [22]), therefore, the decrease of AV-PC fluorescence upon cyt *c* addition at such ionic strength results entirely from the inner filter effect. Comparison of the two types of correction coefficients has revealed that both approaches gave very close estimates of the inner filter effect contribution to the overall changes in donor intensity.

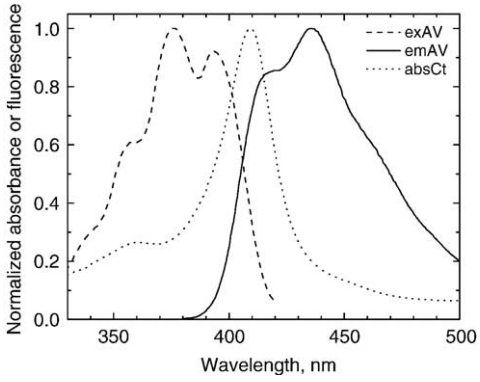


Fig. 3. Normalized fluorescence spectra of anthrylvinyl-phosphatidylcholine in liposomes: excitation (dashed line, $\lambda_{em}$=430 nm) and emission (solid line, $\lambda_{ex}$=375 nm). Also shown is the absorbance spectrum of cytochrome *c* (dotted line).

### 3.5. Förster radius calculation

Critical distance of energy transfer, or Förster radius, for the AV-PC-heme pair was calculated using the expression given by the Förster theory (e.g., [21]):

$$R_0 = \left(\frac{9(\ln 10)}{128\pi^5 N_A}\kappa^2 n_r^{-4}\phi_D J\right)^{\frac{1}{6}},$$
$$J = \int_0^\infty F_D(\lambda)\varepsilon_A(\lambda)\lambda^4 d\lambda \Big/ \int_0^\infty F_D(\lambda)d\lambda, \quad (8)$$

where $N_A$ is the Avogadro number (in mol$^{-1}$), $\kappa^2$ is the orientation factor, $n_r$ is the refractive index of the medium ($n_r$=1.4), $\phi_D$ is the donor quantum yield ($\phi_D$=0.8), and $J$ is the overlap integral calculated from the donor emission spectrum $F_D(\lambda)$ and the acceptor absorption spectrum $\varepsilon_A(\lambda)$ (Fig. 3). Assuming $\kappa^2$ to be 2/3, which is the value obtained for the conditions of isotropic and

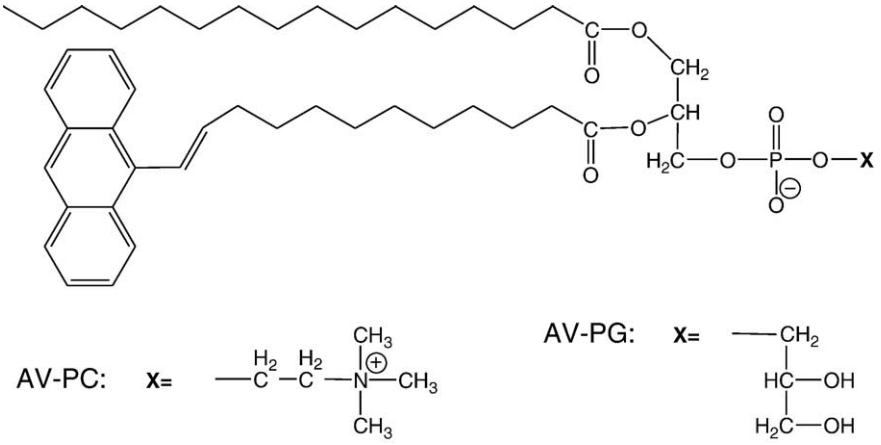


Fig. 2. Chemical structures of the two fluorescent lipid derivatives used as energy donors: anthrylvinyl-phosphatidylcholine (AV-PC) and anthrylvinyl-phosphatidylglycerol (AV-PG).

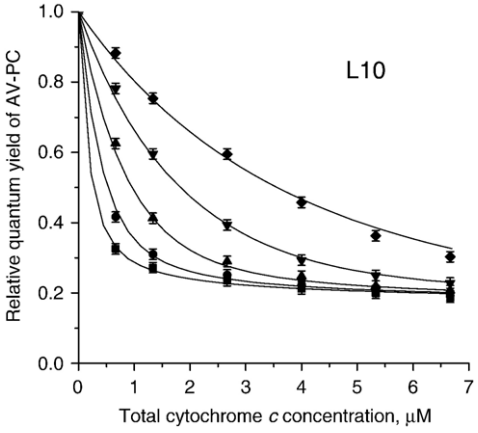


Fig. 4. Concentration dependences of AV-PC fluorescence quenching by cytochrome *c* in liposomes containing 10 mol% CL. Total lipid concentrations: 29 μM (■), 71 μM (●), 143 μM (▲), 285 μM (▼), 571 μM (♦). Solid lines show theoretical curves providing the best global fit of the data.

dynamic averaging of the donor and acceptor transition moment orientations [23], the Förster radius for our donor–acceptor pair is found to be 4.7 nm.

The assumption of $\kappa^2=2/3$ can be shown to provide a close approximation for the system studied here. Indeed, the anthrylvinyl moiety of AV-PC has a considerable orientational freedom in the lipid bilayer which is evidenced by the low anisotropy of 0.054±0.002 for AV-PC in liposomes ($\lambda_{ex}=375$ nm) as compared to the fundamental anisotropy of ca. 0.15 ($\lambda_{ex}=375$ nm, [24]). At the same time, the heme acceptor in cytochrome *c* has degenerate *x*- and *y*-polarized absorption bands [25], which means that its transition moment may have any orientation within the plane of porphyrin ring. In general, the contribution of orientational effects to the efficiency of FRET between chromophores distributed in the membrane can be calculated in a precise way using the approach of Davenport and coworkers [26,27]. Numerical simulations of the energy transfer from AV-PC to the heme of cyt *c* in the membrane have shown that the uncertainty in $R_0$ and hence the uncertainty in any structural parameter derived from the analysis of FRET data depends on the orientation of the cyt *c* heme group with respect to the membrane surface. In the case where the porphyrin ring is parallel to the membrane surface – the orientation suggested by the recent ESR results for cyt *c* [28] – the error of $d_c$ determination due to the assumption of $\kappa^2=2/3$ does not exceed 1%. In the most unfavorable case, where the heme is perpendicular to the membrane surface this assumption results in the underestimation of $d_c$ by less than 8%.

## 4. Results

Fig. 4 shows relative quantum yield of AV-PC fluorescence in PC liposomes containing 10 mol% of acidic lipid cardiolipin (CL). FRET efficiency was recorded as a function of both total protein concentration and total lipid concentration (different curves in Fig. 4) in 5 mM Na-phosphate buffer. AV-PC fluorescence was measured immediately after mixing the liposome suspension and cyt *c* solution, since the fluorescence signal did not change significantly after several seconds of equilibration. Following correction for the inner filter effect, the data were globally analyzed as described previously [14]. In brief, both structural parameter–transverse location of acceptor in the membrane–and binding parameters describing acceptor association with the membrane can be recovered by global analysis of two-dimensional FRET data recorded at different total acceptor and total lipid concentrations. For the analysis, the model of FRET in the membrane is coupled to an adequate adsorption model. In the present study we use the model of energy transfer from a plane of donors to a plane of acceptors [29] in combination with the adsorption model based on scaled particle theory [15,30] as outlined in Theory. Solid lines in Fig. 4 show the best fit obtained during the approximation. Corresponding parameters are given in Table 1 along with 67% confidence intervals and reduced-$\chi^2$ value. Note that in this case $d_c=3.6$ nm stands for the distance between the bilayer midplane and the heme group of cyt *c*. Interestingly, approximations with other adsorption models, e.g., Langmuir model, Van der Waals 2-D gas model [31], or lattice models [32], provided very close values of $d_c$ (data not shown). In particular, global analysis of L10 data within the framework of Langmuir binding model has been performed in [14], giving $K_d=0.28^{+0.09}_{-0.08}$ μM, $n=27\pm2$ and $d_c=3.51\pm0.09$ nm. Both Langmuir and SPT-based binding models give almost identical values of $K_d$ and $d_c$ (cf. Table). At the same time, more than twofold difference in apparent stoichiometry results from the alternative ways to define stoichiometry in the two models: while in Langmuir model a binding site includes all lipid molecules corresponding to one protein molecule (even those not covered by the protein, but sterically excluded from the interaction with other protein molecules), in the SPT model stoichiometry shows the number of lipid molecules that are actually covered by the protein.

Similar experiments have been carried out with liposomes containing higher amounts of CL, 20 and 40 mol%, in the same buffer solution (5 mM Na-phosphate). The data for liposomes with 20 mol% CL (hereafter referred to as L20) are shown in Fig. 5A. The data for liposomes containing 40 mol% CL (L40) are qualitatively similar to L20 and are not shown here. Additionally, FRET efficiency in liposomes with 20 mol% of CL was measured in the presence of 15 and 30 mM NaCl (Fig. 5B and C; datasets L20/S15 and L20/S30, respectively). Protein solutions and liposome suspensions for these experiments were prepared

Table 1
Results of nonlinear least-squares global fit of FRET data obtained under different experimental conditions

| Dataset | CL content, mol% | Ionic strength, mM $Na^+$ | Fitting parameters | | | $\chi^2_R$ |
|---|---|---|---|---|---|---|
| | | | $n_{pm}$ | $K_d$, μM | $d_c$, nm | |
| L10 | 10 | 5 | $11.9^{+0.9}_{-0.4}$ | $0.31^{+0.13}_{-0.11}$ | $3.55^{+0.06}_{-0.07}$ | 0.837 |
| L20 | 20 | 5 | 4.1±4.1 | $0.008^{+9.73}_{-0.008}$ | $4.24^{+0.14}_{-0.12}$ | 10.8 |
| L20/S15 | 20 | 20 | $6.8^{+1.0}_{-0.9}$ | $0.18^{+0.22}_{-0.1}$ | $3.94^{+0.9}_{-0.7}$ | 0.746 |
| L20/S30 | 20 | 35 | $6.5^{+0.9}_{-0.8}$ | $4.54^{+1.49}_{-1.04}$ | 4.09±0.1 | 0.778 |
| L40 | 40 | 5 | 2.9±2.9 | $0.001^{+1.53}_{-0.001}$ | 4.30±0.13 | 11.46 |

Confidence intervals (calculated for 67% confidence level) and reduced chi-square values are given for each fit.

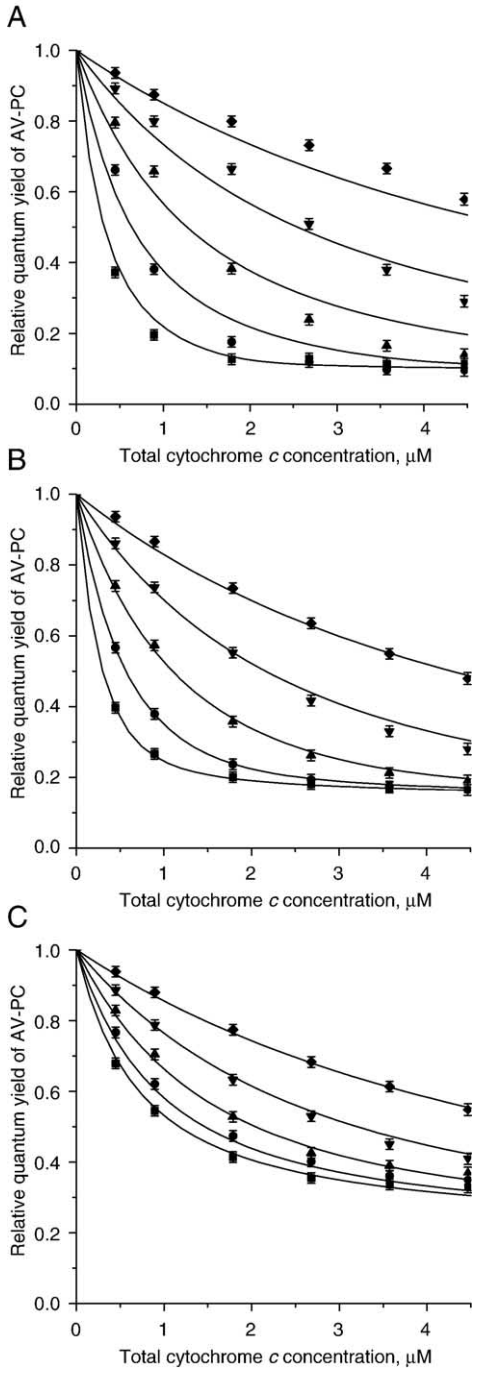


Fig. 5. Concentration dependences of AV-PC fluorescence quenching by cytochrome *c* in liposomes containing 20 mol% CL. Experiments were carried out in 5 mM Na-phosphate buffer (A) and in the same buffer with the addition of 15 mM NaCl (B) or 30 mM NaCl (C). Total lipid concentrations: 33 μM (■), 66 μM (●), 132 μM (▲), 263 μM (▼), 527 μM (♦). Solid lines show theoretical curves providing the best global fit of the data.

in 5 mM Na-phosphate buffer containing specified amounts of salt.

Global analysis of datasets L20 and L40 has shown that these data cannot be satisfactorily fitted by the FRET model in combination with various adsorption models. The best attainable approximation is shown in Fig. 5A with solid lines. Corresponding parameters are given in Table 1. Note the vast confidence intervals for binding parameters and large values of $\chi_R^2 >> 1$. Although $d_c$ values obtained for these data have quite narrow confidence intervals, they should only be considered as effective, averaged values.

In order to understand which features of data L20 and L40 account for the difference between the experiment and the theoretical prediction, these data have been analyzed qualitatively and compared with the data obtained for liposomes with 10 mol% CL (L10). As can be seen in Figs. 4 and 5A, increase of the CL content in liposomes leads to lowering of the saturation level of AV-PC relative quantum yield. Saturation of energy transfer efficiency occurs at high protein/lipid ratios when the full coverage of membrane surface with adsorbed cyt *c* is approached. Since energy transfer efficiency in membranes depends both on the acceptor surface density and on the distance of closest approach between donors and acceptors (which in our case corresponds to the distance between the donor and acceptor planes, Fig. 1), the enhancement of FRET at saturation may correspond to more dense packing of the protein molecules at the membrane surface and/or deeper protein penetration into the bilayer.

The characteristic feature of L20 and L40 data, as compared with L10, is the reduced energy transfer at high lipid concentrations, which is reflected by the elevation of the two upper curves in Fig. 5A with respect to the equivalent curves in Fig. 4 (if the differences in the lipid concentrations in L20 and L10 are taken into account, the elevation will be even larger). Such behavior is rather unexpected since cyt *c* affinity to phospholipid membranes is known to increase with anionic lipid content (e.g., [33]), and thus FRET efficiency should rise with cardiolipin content (at fixed protein and lipid concentrations).

It is also interesting to analyze the changes of energy transfer in liposomes containing 20 mol% of CL that occur at higher ionic strengths (cf. Fig. 5A–C). In accordance with

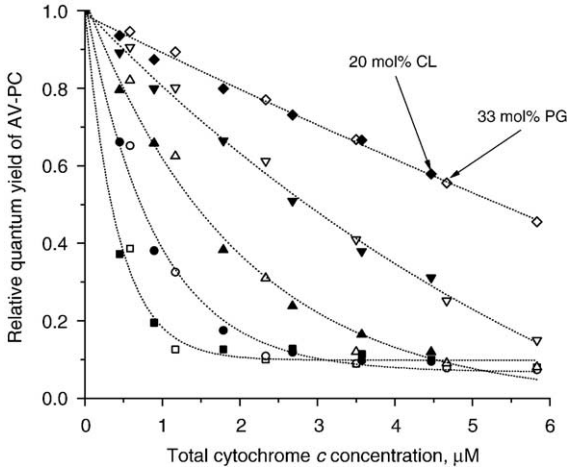


Fig. 6. Comparison of AV-PC quenching profiles obtained in liposomes containing 20 mol% cardiolipin (filled symbols) or 33 mol% phosphatidylglycerol (open symbols) under low ionic strength conditions. Total concentrations of lipid expressed in terms of acyl chain pairs: 39 μM (■), 79 μM (●), 157 μM (▲), 314 μM (▼), 628 μM (♦). Dotted lines are for guidance only and have no theoretical significance.

other studies [12,33] and with the conception of electrostatic (initial) binding of cyt *c* to charged membranes, data in Fig. 5A–C demonstrate lowering of the protein affinity (namely, the equilibrium binding constant) for the membrane in response to the ionic strength elevation. In contrast to L20, data obtained at higher ionic strength (L20/S15 and L20/S30) can be fitted by Eqs. (1)–(6) fairly well. Structural and binding parameters obtained by the global analysis are listed in Table 1. It is evident that the agreement between the models and the experimental data is very good (Fig. 5B, C; $\chi_R^2<1$), and the obtained parameters confirm the qualitative conclusions made above. Indeed, the equilibrium dissociation constant ($K_d$) and the effective binding stoichiometry ($n_{pm}$, per monolayer) increase monotonically with ionic strength (Table 1).

To address possible role of specific properties of cardiolipin molecule in the unexpected behavior of L20 and L40 data, we performed similar measurements in liposomes containing phosphatidylglycerol (PG) instead of cardiolipin. Due to its effective shape, the CL molecule has a propensity for non-bilayer structures [34,35], and cyt *c* was in fact shown to induce the $H_{II}$ phase formation in CL-containing liposomes [36]. Meanwhile, phosphatidylglycerol does not produce curvature strain in the membrane and thus forms stable bilayers. In terms of the number of aliphatic chains and phosphate groups one CL molecule may be considered approximately equivalent to two PG molecules, then 20 mol% of CL will correspond to 33 mol% of PG. The fluorescence data obtained under the same conditions with PC/CL liposomes (20 mol% CL, the same data as in Fig. 5A) and PC/PG liposomes (33 mol% PG, G33 data) are compared in Fig. 6. As can be seen in the figure, the data obtained with PG and CL are very close suggesting no significant influence of CL non-bilayer forming properties on our energy transfer data. It is also worth noting that the goodness of fit for G33 data is even worse than for L20 data.

Finally, to assess how the FRET data can be affected by electrostatic phenomena, such as nonuniform distribution of donors and acceptors originating from the interactions between positively charged cyt *c* molecule and the acidic lipid component, additional measurements have been performed with negatively charged fluorescent lipid analog anthrylvinyl-phosphatidylglycerol (AV-PG) instead of AV-PC. Comparison of fluorescence data obtained in liposomes with identical compositions (PC/PG, 33 mol% PG) but with donor fluorophore attached either to zwitterionic PC or to anionic PG is made in Fig. 7. Again, the two datasets are seen to be virtually indistinguishable from each other implying no significant contribution of membrane component electrostatic demixing to the FRET concentration dependences.

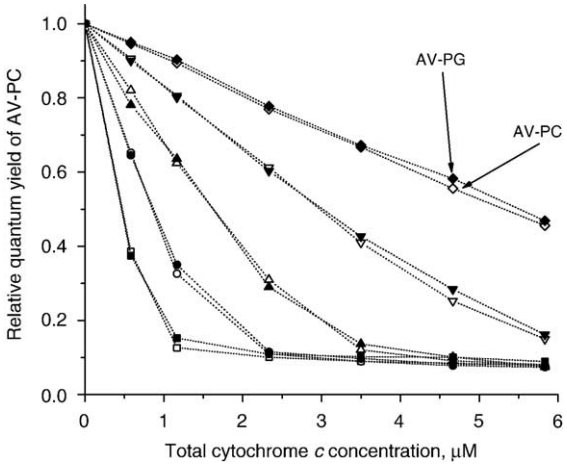


Fig. 7. Comparison of AV-PC (open symbols) and AV-PG (filled symbols) quenching profiles obtained on liposomes containing 33 mol% phosphatidylglycerol under low ionic strength conditions. Total concentrations of lipid expressed in terms of acyl chain pairs: 39 μM (■), 79 μM (●), 157 μM (▲), 314 μM (▼), 628 μM (♦).

## 5. Discussion

### 5.1. Membrane location of cyt c at low CL content

Cyt *c* binding to negatively charged membranes is known to evoke appreciable destabilization or partial unfolding of cyt *c* at the level of tertiary structure (e.g., [6,37,38]). Indeed, denaturation temperature [37,39] as well as resistance to urea denaturation [40] have been shown to decrease substantially upon binding. Dramatic enhancement of hydrogen–deuterium exchange observed for cyt *c* bound to phosphatidylserine [41] or phosphatidylglycerol [39] membranes reveals increased accessibility of the protein backbone amide groups to solvent. Pinheiro and co-workers [41] have shown that the transition from tightly packed native structure to partially denatured state is a highly concerted global transition that exposes all amides of the protein core to solvent. Interestingly, the major part of the evidences for cyt *c* unfolding have been obtained with model membranes composed entirely of anionic lipid, while it has been shown that the degree of destabilization increases with the anionic lipid content [37,42]. To examine the extent of perturbations in cyt *c* structure occurring in our experiments we recorded absorbance and fluorescence spectra of the protein in the presence of liposomes (under conditions of the FRET experiments) and compared them to corresponding solution spectra (data not shown). Changes in Soret absorbance did not exceed 7% and were presumably due to incomplete correction for liposome scattering, which was accomplished by subtracting vesicle turbidity spectra from the corresponding absorbance spectra of cyt *c* in the presence of liposomes. Moreover, no intrinsic fluorescence of cyt *c* was detected in the presence of liposomes with urea-denatured protein as a positive control, which indicates that no large-scale unfolding of polypeptide chain occurs and $Trp_{59}$ fluorescence remains to be quenched by the heme (cf. [38]). Therefore, it is assumed here that, in spite of the loosening of its tertiary structure, cyt *c* bound to mixed membranes with low anionic lipid content under our experimental conditions retains its globular structure and main features of the 3D fold. This relatively compact membrane-bound state of cyt *c* is close to the molten globule state observed at low pH [43].

As mentioned above, the estimate of $d_c=3.6$ nm obtained by the global analysis of the L10 data represents the distance between the heme group of cyt *c* and the bilayer midplane

(Fig. 1). According to the solution structure of cytochrome *c* [44] the protein has spheroidal shape with dimensions $3\times3.4\times3.4$ nm, and the heme group is displaced off the molecule center by a distance $r_t \sim 0.7$ nm. As can be seen from Fig. 1, the bounds for the depth of protein penetration in the bilayer ($D_P$) can be found by considering two orientations where the heme group lies above or below the molecule center at the normal to the membrane that runs through the protein center. Then, the lower and upper bounds for $D_P$ are $D_P^{min,max}=0.5d_m-d_c+R_P^{*}\mp r_t$, where $R_P^{*}$ is the effective radius of the protein in the lipid-bound state. Assuming that the bound cyt *c* has a molten globule-like structure and taking into account that the radius of gyration for the A-state of cyt *c* is approximately 30% greater than the value for the native structure [45], an estimate for $R_P^{*}$ can be calculated by multiplying the average radius of the native structure (~1.6 nm) by a factor of 1.3 to yield $R_P^{*} \approx 2.1$ nm. Then, using this value along with $d_m \approx 4.5$ for eggPC bilayer [46] we obtain $D_P^{min} \approx 0.1$ nm and $D_P^{max} \approx 1.5$ nm, i.e., depending on the actual orientation of the protein L10 data may be interpreted in terms of either adsorption at the bilayer surface ($D_P \sim 0$) or insertion up to the level of initial methylenes.

In the next section, the analysis of the data obtained with higher cardiolipin content (L20 and L40) will be performed, suggesting that distance $d_c$ may vary with experimental conditions reaching in the extreme cases a maximum value of ~4.6 nm. It is tempting to assume that this maximum $d_c$ value corresponds to the loosest possible binding of cyt *c* to the membrane, when the protein touches the membrane surface without penetrating it. If the protein orientation with respect to the bilayer surface remains unchanged, then in a similar manner $d_c=3.6$ nm will correspond to the depth of protein penetration of ~1 nm. Cyt *c* orientation giving rise to such relationship between $d_c$ and $D_P$ is depicted in Fig. 1. The side of cyt *c* molecule that is turned to the membrane contains $Lys_{72}$, $Lys_{73}$, $Lys_{86}$, $Lys_{87}$ and $Met_{65}$. Interestingly, this is in close agreement with recent ESR results showing that cyt *c* binds to DOPG bilayers with the side on which $Lys_{86}$, $Lys_{87}$ and $Lys_{72}$ are located [28]. This orientation is also consistent with the NMR and ESR data [47] suggesting that $Met_{65}$ is oriented towards the membrane and shielded from the external solution, as well as the fluorescence data [7,48] pointing to the accessibility of the exposed heme edge to the solvent. In another fluorescence study, it was proposed that conserved lysines 72 and 73 were involved in cyt *c* binding to deprotonated acidic lipids [22]. Hence, with the above assumption on the protein orientation, our FRET data for liposomes with 10 mol% CL suggest that cyt *c* is inserted in the bilayer to the level of carbonyls or initial methylenes.

### 5.2. Structural rearrangements of cyt c–lipid complexes.

On the contrary to L10 data, the results obtained with higher acidic phospholipid content at low ionic strength cannot be fitted by conventional adsorption models and the model of FRET for donors and acceptors uniformly distributed in planes separated by a fixed distance (Table 1). Therefore, some structural rearrangements in the lipid–protein complexes must be involved that change the donor–acceptor separation as a function of: (i) cardiolipin content, (ii) lipid concentration or the ratio of total lipid and protein concentrations, L/P and (iii) ionic strength of the medium.

In Fig. 8, datasets L10, L20, and L40 are presented as dependences of relative quantum yield of AV-PC on surface density of cyt *c* on the membrane. Such representation is very convenient for the analysis of the geometrical changes in the donor–acceptor system depending on the extent of membrane coverage with protein. These plots were obtained by using the effective binding parameters for cyt *c* in corresponding membrane systems. The parameters for L10 data were taken from the results of the global analysis (Table 1), while the parameters for L20 and L40 were obtained from global analysis of the data points that lie below the $Q_r$ level of ~0.2, i.e. in the region of incomplete protein binding. Theoretical curves in Fig. 8 were calculated using Eqs. (1)–(6). Comparison of the experimental data with the theoretical curves leads to the following conclusions: (i) L10 data are fitted fairly well by theory with $d_c=3.6$ nm in the whole range of the protein surface density; (ii) at low surface densities ($C_A^s \leq 0.025$ nm$^{-2}$) L20 and L40 data can be described by theory with $d_c=4.6$ nm; iii) at high surface densities ($C_A^s \geq 0.07$ nm$^{-2}$) L20 and L40 data can be described by theory with $d_c=3.6$ nm; iv) at intermediate surface densities ($0.025 \leq C_A^s \leq 0.07$ nm$^{-2}$) $d_c$ changes continuously from 4.6 down to 3.6 nm. Hence, this semi-quantitative analysis suggests that in the range of cyt *c* surface densities between ~0.025 and ~0.07 the structure of the protein–lipid membrane with high CL content alters in such a way that the distance of closest approach between donors and acceptors decreases from 4.6 to 3.6 nm.

It should be noted that we had attempted similar quantitative analysis of FRET data in the system cytochrome *c*-liposomes previously. Based on the limited experimental data with

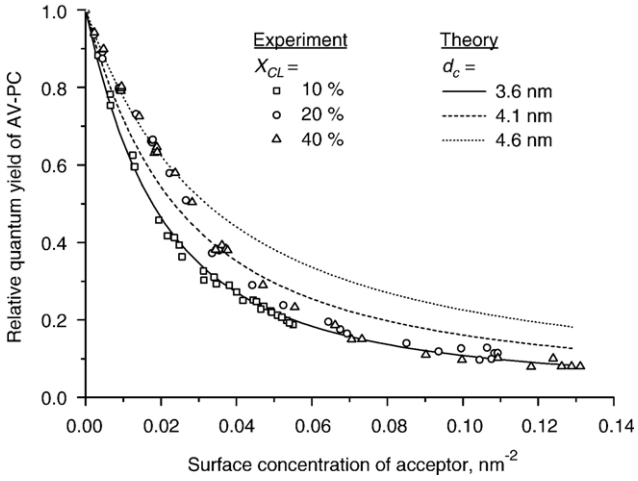


Fig. 8. Dependences of AV-PC fluorescence quenching on the surface density of membrane bound cytochrome *c*: comparison of the liposomes containing 10 mol% CL (squares), 20 mol% CL (circles) or 40 mol% CL (triangles). Theoretical curves were calculated using different distances between the bilayer midplane and the level of cyt *c* heme groups: $d_c=3.6$ nm (solid line), $d_c=4.1$ nm (dashed line) and $d_c=4.6$ nm (dotted line).

amphiphilic membrane probe 3-methoxybenzanthrone as energy donor, no clear trend was evident in the depth of cyt *c* penetration in the bilayer depending on the CL content (10, 50, or 80 mol%). In the present study, we utilized the advanced global analysis methodology applied to the expanded experimental dataset in order to improve the reliability of the quantitative analysis and to narrow down the uncertainties in the recovered structural parameters. Moreover, by using a fluorescent lipid analog as donor, we were able to perform FRET measurements in a more defined system from the viewpoint of the donor localization within the bilayer.

Various rearrangements of protein–lipid membranes discussed in the literature on the peripheral protein interactions with membranes can be classified as shown in Fig. 9. Firstly, binding of charged protein to the membrane composed of a mixture of neutral and (oppositely) charged lipids can cause lateral redistribution of the components due to migration of the charged lipid species to the protein adsorption site [30]. Numerical calculations [49] show that the magnitude of local deviations in charged lipid density is determined by the balance between attractive electrostatic interactions and mixing entropy. Their results indicate that the local demixing can be substantial in the case where strongly charged protein adsorbs on weakly charged membrane. Another mechanism of protein–lipid lateral redistribution is the formation of macroscopic domains of adsorbed protein, which has been observed experimentally upon adsorption of cytochrome *c* [50] or cationic peptides [51] on mixed phospholipid membranes. Accordingly, similar phenomena may be expected to occur in our experiments. In this case, anionic CL would concentrate in the vicinity of adsorbed cyt *c* thus displacing the zwitterionic species, including AV-PC, from the protein vicinity, which would result in the reduction of energy transfer. However, our experiments with anionic energy donor, AV-PG, have proven that our data are not affected by the electrostatic redistribution of lipid or protein components (Fig. 7). Indeed, if the lateral redistribution of the membrane components affected our FRET data, in the experiment with AV-PG at small $B/L$ we would see the increase in the FRET efficiency relative to the level predicted for uniform distributions of donors and acceptors, which is the opposite to the effect observed in experiments with AV-PC (Fig. 5A). The insensitivity of our data to possible lateral redistribution could be explained, in part, by the fact that AV-PC donors in the inner liposome leaflet retain uniform distribution and smooth out the effect of lipid demixing in the outer leaflet.

The second type of possible structural rearrangements is the formation of non-bilayer structures. This phenomenon may also affect the energy transfer from AV-PC to cyt *c*. If the CL molecules concentrate in the regions with negative curvature, i.e., in the nonbilayer structures around cyt *c* molecules, the displacement of AV-PC molecules from the protein vicinity can take place, leading to the reduction of FRET. However, our results with PG used instead of CL rule out this possibility (Fig. 6).

The third type of rearrangements is the changes of the protein transverse position in the bilayer depending on its surface density. The results of additional experiments shown in Figs. 6 and 7 suggest that it is the only possible rearrangement of the protein lipid membrane that is consistent with FRET data. Hence, it can be concluded that in a certain range of cyt *c* surface concentrations (approximately from 0.02 to 0.07 $nm^{-2}$) interfacially bound protein inserts deeper into the bilayer resulting in the apparent reduction of $d_c$ by ~1 nm. It should be noted that such behavior is observed only at high acidic phospholipid content (>10 mol% CL) and low ionic strength of the medium (<20 mM $Na^+$).

It is now widely accepted that following electrostatic binding to the bilayer surface some peripheral proteins are capable of inserting into the hydrophobic core of the membrane [52]. Similar phenomena are observed on binding of cytolytic and antimicrobial peptides to membranes (e.g., [53,54]), which at a certain critical concentration insert into the bilayer and form aqueous pores. To describe such a situation Zuckermann and Heimburg [11] developed a theoretical formalism based on the Minton's theory for surface adsorption of the ligand that may have different conformations or aggregate at the surface

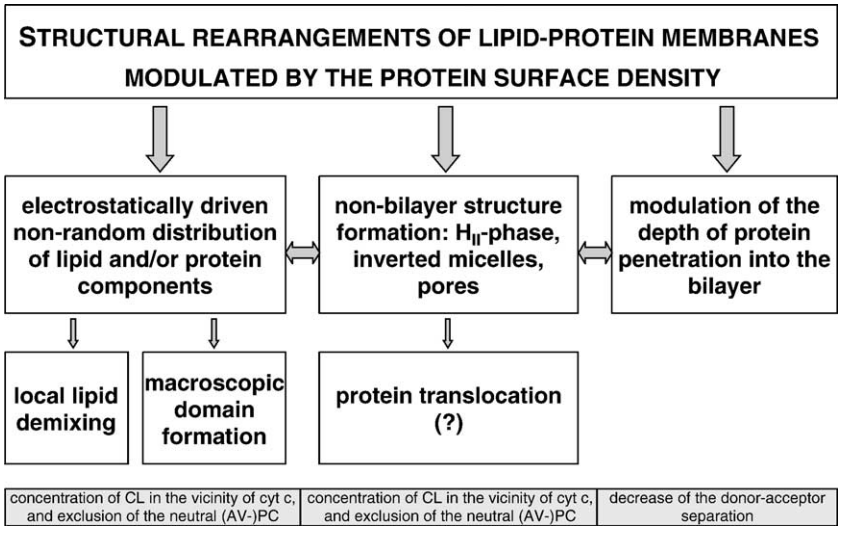


Fig. 9. Diagram of possible structural rearrangements of lipid–protein membranes and their relations. Relevant literature references are given in the text.

[15,55]. According to this formalism, protein molecules adsorbed at the lipid–water interface form the 2-D gas, which exerts lateral pressure on the bilayer lipid membrane. At high surface densities, this pressure can become high enough to overcome the energy barrier for protein insertion [11]. The protein concentration at which the insertion begins is a function of the membrane line tension, i.e., the additional energy imparted to lipids around the inserted protein. Line tension, in turn, is related to the protein shape and properties as well as with the spontaneous curvatures of membrane constituents, which in the case of charged lipids depends, among other factors, on the ionic strength and pH of aqueous medium [11,56]. The authors of [11] have applied this formalism to the experimental data of Heimburg and Marsh [31], which had been obtained for cyt *c* binding to DOPG membranes at various ionic strength in the range 0–250 mM $Na^+$ using ultracentrifugation. At ionic strengths lower than 40 mM $Na^+$ unusual binding isotherms were observed suggesting that some changes in the mode of protein binding occurred at low ionic strength. Subsequent ESR [31] and titration calorimetry [11] experiments revealed that the change in mode of binding is most likely a result of cyt *c* insertion into the bilayer due the increase in protein surface concentration. Interestingly, in our FRET experiments, the unusual behavior of concentration dependences for the efficiency of energy transfer to cyt *c* was observed in the same range of ionic strengths of 0–35 mM $Na^+$ (data L20, L20/S15, and L20/S30). In addition, experimental data supporting the insertion of cyt *c* into the charged membranes have been recently obtained using viscosity and turbidity measurements, resonance Raman, circular dichroism, and UV/vis absorption spectroscopy [57] as well as by direct atomic force microscopy [9].

In conclusion, our work demonstrates that steady state FRET can be applied as a quantitative tool for monitoring the changes in molecular organization of protein–lipid assemblies. In particular, FRET data suggest that at low ionic strength the depth of cytochrome *c* penetration into the bilayer is modulated by the protein surface concentration. The extent of the protein insertion into the membrane is determined by the ionic strength of solution and the membrane acidic phospholipid content. Further details of structural reorganizations taking place in the cytochrome *c*–lipid complexes could be revealed by time-resolved FRET measurements, which are known to be particularly well suited for distinguishing different types of donor–acceptor distance distributions (e.g., [21]). This work is currently planned by our group.

## Acknowledgements

We are very grateful to Drs. A. D. Roshal and A. O. Doroshenko for the use of fluorescence facilities (Kharkiv National University).

## References

[1] J. Berg, J. Tymoczko, L. Stryer, Biochemistry, 5th ed., W.H. Freeman and Co, New York, 2002.
[2] S.S. Gupte, C.R. Hackenbrock, Multidimensional diffusion modes and collision frequencies of cytochrome *c* with its redox partners, J. Biol. Chem. 263 (1988) 5241–5247.
[3] X.J. Jiang, X.D. Wang, Cytochrome *c*-mediated apoptosis, Annu. Rev. Biochem. 73 (2004) 87–106.
[4] H. Zhao, E.K. Tuominen, P.K. Kinnunen, Formation of amyloid fibers triggered by phosphatidylserine-containing membranes, Biochemistry 43 (2004) 10302–10307.
[5] J.D. Cortese, A.L. Voglino, C.R. Hackenbrock, Multiple conformations of physiological membrane-bound cytochrome *c*, Biochemistry 37 (1998) 6402–6409.
[6] S. Bernad, S. Oellerich, T. Soulimane, S. Noinville, M.H. Baron, M. Paternostre, S. Lecomte, Interaction of horse heart and thermus thermophilus type c cytochromes with phospholipid vesicles and hydrophobic surfaces, Biophys. J. 86 (2004) 3863–3872.
[7] J. Teissie, Interaction of cytochrome c with phospholipid monolayers. Orientation and penetration of the protein as a function of the packing density of film, nature of phospholipids and ionic content of the aqueous phase, Biochemistry 20 (1981) 1554–1560.
[8] Z. Salamon, G. Tollin, Surface plasmon resonance studies of complex formation between cytochrome *c* and bovine cytochrome c oxidase incorporated into a supported planar lipid bilayer: I. Binding of cytochrome *c* to cardiolipin/phosphatidylcholine membranes in the absence of oxidase, Biophys. J. 71 (1996) 848–857.
[9] E.J. Choi, E.K. Dimitriadis, Cytochrome *c* adsorption to supported, anionic lipid bilayers studied via atomic force microscopy, Biophys. J. 87 (2004) 3234–3241.
[10] M. Schlame, D. Rua, M.L. Greenberg, The biosynthesis and functional role of cardiolipin, Prog. Lipid Res. 39 (2000) 257–288.
[11] M.J. Zuckermann, T. Heimburg, Insertion and pore formation driven by adsorption of proteins onto lipid bilayer membrane–water interfaces, Biophys. J. 81 (2001) 2458–2472.
[12] M. Rytömaa, P.K.J. Kinnunen, Evidence for two distinct acidic phospholipid-binding sites in cytochrome *c*, J. Biol. Chem. 269 (1994) 1770–1774.
[13] G.P. Gorbenko, Ye.A. Domanov, Cytochrome *c* location in phosphatidylcholine/cardiolipin model membranes: resonance energy transfer study, Biophys. Chemist. 103 (2003) 239–249.
[14] Ye.A. Domanov, G.P. Gorbenko, J.G. Molotkovsky, Global analysis of steady-state energy transfer measurements in membranes: resolution of structural and binding parameters, J. Fluoresc. 14 (2004) 49–55.
[15] R. Chatelier, A.P. Minton, Adsorption of globular proteins on locally planar surfaces: models for the effect of excluded surface area and aggregation of adsorbed protein on adsorption equilibria, Biophys. J. 71 (1996) 2367–2374.
[16] S. Batzri, E. Korn, Single bilayer liposomes prepared without sonication, Biochim. Biophys. Acta 298 (1973) 1015–1019.
[17] G.R. Bartlett, Phosphorus assay in column chromatography, J. Biol. Chem. 234 (1959) 466–468.
[18] J.G. Molotkovsky, P.I. Dmitriev, L.F. Nikulina, L.D. Bergelson, Synthesis of new fluorescent labeled phosphatidylcholines, Bioorg. Khim. 5 (1979) 588–594.
[19] J.G. Molotkovsky, M.M. Smirnova, M.O. Karyukhina, L.D. Bergelson, Synthesis of anthrylvinyl phospholipids probes, Russ. J. Bioorgan. Chem. 15 (1989) 377–380.
[20] L.D. Bergelson, J.G. Molotkovsky, Y.M. Manevich, Lipid-specific probes in studies of biological membranes, Chem. Phys. Lipids 37 (1985) 165–195.
[21] J.R. Lakowicz, Principles of Fluorescent Spectroscopy, 2nd ed., Plenum Press, New York, 1999.
[22] M. Rytömaa, P.K.J. Kinnunen, Reversibility of the binding of cytochrome *c* to liposomes. Implications for lipid–protein interactions, J. Biol. Chem. 270 (1995) 3197–3202.
[23] R. Dale, J. Eisinger, W. Blumberg, The orientational freedom of molecular probes. The orientation factor in intramolecular energy transfer, Biophys. J. 26 (1979) 161–194.
[24] L.B. Johansson, J.G. Molotkovsky, L.D. Bergelson, Fluorescence properties of anthrylvinyl lipid probes, Chem. Phys. Lipids 53 (1990) 185–189.

[25] W.A. Eaton, R.M. Hochstrasser, Electronic spectrum of single crystals of ferricytochrome-*c*, J. Chem. Phys. 46 (1967) 2533–2539.
[26] L. Davenport, R. Dale, R. Bisby, R. Cundall, Transverse location of the fluorescent probe 1,6-diphenyl-1,3,5-hexatriene in model lipid bilayer membrane systems by resonance excitation energy transfer, Biochemistry 24 (1985) 4097–4108.
[27] Ye.A. Domanov, G.P. Gorbenko, Analysis of resonance energy transfer in model membranes: role of orientational effects, Biophys. Chemist. 99 (2002) 143–154.
[28] A. Kostrzeva, T. Páli, W. Froncisz, D. Marsh, Membrane location of spin-labeled cytochrome *c* determined by paramagnetic relaxation agents, Biochemistry 39 (2000) 6066–6074.
[29] G.P. Gorbenko, Ye.A. Domanov, Energy transfer method in membrane studies: some theoretical and practical aspects, J. Biochem. Biophys. Methods 52 (2002) 45–58.
[30] T. Heimburg, B. Angerstein, D. Marsh, Binding of peripheral proteins to mixed lipid membranes: effect of lipid demixing upon binding, Biophys. J. 76 (1999) 2575–2586.
[31] T. Heimburg, D. Marsh, Protein surface distribution and protein–protein interactions in the binding of peripheral proteins to charged lipid membranes, Biophys. J. 68 (1995) 5436–5546.
[32] S. Stankowski, Large ligand adsorption to membranes: II. Disc-like ligands and shape dependence at low saturation, Biochim. Biophys. Acta 735 (1983) 352–360.
[33] M. Rytömaa, P. Mustonen, P.K.J. Kinnunen, Reversible, nonionic, and pH-dependent association of cytochrome *c* with cardiolipin-phosphatidylcholine liposomes, J. Biol. Chem. 267 (1992) 22243–22248.
[34] R.P. Rand, S. Sengupta, Cardiolipin forms hexagonal structures with divalent cations, Biochim. Biophys. Acta 255 (1972) 484–492.
[35] B. de Kruijff, P.R. Cullis, A.J. Verkleij, M.J. Hope, C.J.A. van Echteld, T.F. Taraschi, P. van Hoogevest, J.A. Killian, A. Rietveld, A.T.M. van der Steen, Modulation of lipid polymorphism by lipid–protein interactions, in: A. Watts, J.J.H.H.M. de Pont (Eds.), Progress in Protein–Lipid Interactions, Elsevier, Amsterdam, 1985, pp. 89–142.
[36] B. de Kruijff, P.R. Cullis, Cytochrome *c* specifically induces hexagonal non-bilayer structures in cardiolipin-containing model membranes, Biochim. Biophys. Acta 602 (1980) 477–490.
[37] A. Muga, H.H. Mantsch, W.K. Surewicz, Membrane binding induces destabilization of cytochrome *c* structure, Biochemistry 30 (1991) 7219–7224.
[38] T.J.T. Pinheiro, G.A. Elöve, A. Watts, H. Roder, Structural and kinetic description of cytochrome *c* unfolding induced by the inter-action with lipid vesicles, Biochemistry 36 (1997) 13122–13132.
[39] T. Heimburg, D. Marsh, Investigation of secondary and tertiary structural changes of cytochrome *c* in complexes with anionic lipids using amide hydrogen exchange measurements: an FTIR study, Biophys. J. 65 (1993) 2408–2417.
[40] H. de Jongh, J. Killian, B. de Kruijff, A water–lipid interface induces a highly dynamic folded state in apocytochrome *c* and cytochrome *c* which may represent a common folding intermediate, Biochemistry 31 (1992) 1636–1643.
[41] T.J.T. Pinheiro, H. Cheng, S.H. Seeholzer, H. Roder, Direct evidence for the cooperative unfolding of cytochrome c in lipid membranes from H–$^{2}$H exchange kinetics, J. Mol. Biol. 303 (2000) 617–626.
[42] T.J.T. Pinheiro, The interaction of horse heart cytochrome *c* with phospholipid bilayers. Structural and dynamic effects, Biochimie 76 (1994) 489–500.
[43] V.E. Bychkova, A.E. Dujsekina, S.I. Klenin, E.I. Tiktopulo, V.N. Uversky, O.B. Ptitsyn, Molten globule-like state of cytochrome *c* under conditions simulating those near the membrane surface, Biochemistry 35 (1996) 6058–6063.
[44] L. Banci, I. Bertini, H.B. Gray, C. Luchinat, T. Reddig, A. Rosato, P. Turano, Solution structure of oxidized horse heart cytochrome *c*, Biochemistry 36 (1997) 9867–9877 (1AKK).
[45] S. Akiyama, S. Takahashi, T. Kimura, K. Ishimori, I. Morishima, Y. Nishikawa, T. Fujisawa, Conformational landscape of cytochrome *c* folding studied by microsecond-resolved small-angle X-ray scattering, Proc. Natl. Acad. Sci. U. S. A. 99 (2002) 1329–1334.
[46] J.F. Nagle, S. Tristram-Nagle, Structure of lipid bilayers, Biochim. Biophys. Acta 1469 (2000) 159–195.
[47] L. Brown, K. Wüthrich, NMR and ESR studies of the interactions of cytochrome *c* with mixed cardiolipin-phosphatidylcholine vesicles, Biochim. Biophys. Acta 468 (1977) 389–410.
[48] L.S. Kaminsky, J.J. Henderson, K.M. Ivanetich, Fluorescence studies of a cytochrome *c* mixed phospholipid complex, Biochem. Biophys. Res. Commun. 51 (1973) 40–45.
[49] S. May, D. Harries, A. Ben-Shaul, Lipid demixing and protein–protein interactions in the adsorption of charged proteins on mixed membranes, Biophys. J. 79 (2000) 1747–1760.
[50] D. Haverstick, M. Glaser, Influence of proteins on the reorganization of phospholipid bilayers into large domains, Biophys. J. 55 (1989) 677–682.
[51] G. Denisov, S. Wanaski, M. Glaser, S. McLaughlin, Binding of basic peptide to membranes produces lateral domains enriched in the acidic lipids phosphatidylserine and phosphatidylinositol 4,5-biphosphate: an electrostatic model and experimental results, Biophys. J. 74 (1998) 731–744.
[52] M. Sankaram, D. Marsh, Protein–lipid interactions with peripheral membrane proteins, in: A. Watts (Ed.), Protein–Lipid Interactions, Elsevier, Amsterdam, 1993, pp. 127–162.
[53] A. Ladokhin, M. Selsted, S. White, Bilayer interactions of indolicidin, a small antimicrobial peptide rich in tryptophan, proline and basic amino acids, Biophys. J. 72 (1997) 794–805.
[54] K. Matsuzaki, S. Yoneyama, K. Miyajima, Pore formation and translocation of melittin, Biophys. J. 73 (1997) 831–838.
[55] A.P. Minton, Adsorption of globular proteins on locally planar surfaces: II. Models for the effect of multiple adsorbate conformations on adsorption equilibria and kinetics, Biophys. J. 76 (1999) 176–187.
[56] N. Dan, S.A. Safran, Effect of lipid characteristics on the structure of transmembrane proteins, Biophys. J. 75 (1998) 1410–1414.
[57] S. Oellerich, S. Lecomte, M. Paternostre, T. Heimburg, P. Hildebrandt, Peripheral and integral binding of cytochrome *c* to phospholipid vesicles, J. Phys. Chem., B 108 (2004) 3871–3878.